Journal of Chemical Health Risks
www.jchr.org
JCHR (2025) 15(5), 3495-3502 | ISSN:2251-6727

Facile Green Synthesis and Photocatalytic Efficiency of Ag-Zn Bimetallic Nanoparticles for Degradation of Methylene Blue

Ch. S. Anuradha[1], Ch. Shanthi Devi[2], R. Haritha[3], M. V. Mani Varma[4], M. Hashrita Mani Sree[5]

[1] Department of Chemistry, Dr. V. S. Krishna Government Degree & PG College (Autonomous), Visakhapatnam, Andhra Pradesh.

[2] Department of Microbioloy, Dr. V. S. Krishna Government Degree & PG College (Autonomous), Visakhapatnam, Andhra Pradesh.

[3] Department of Biotechnology, Government Degree College (Men), Srikakulam, Andhra Pradesh.

[4] Centre for Distance and Online Education, Andhra University, Visakhapatnam, Andhra Pradesh.

[5] GITAM Institute of Medical Sciences and Research (GIMSR), Visakhapatnam, Andhra Pradesh.

(Received: 05 September 2025 Revised: 15 September 2025 Accepted: 23 October 2025)

KEYWORDS

Ag–Zn bimetallic nanoparticles, green synthesis, Achyranthes aspera, photocatalytic degradation, methylene blue.

ABSTRACT:

A sustainable plant-mediated approach was adopted for the synthesis of Ag–Zn bimetallic nanoparticles (BMNPs) utilizing Achyranthes aspera leaf extract as an eco-friendly reducing and surface-stabilizing agent. The successful formation of nanoparticles was evidenced by UV-Visible spectroscopy through distinct surface plasmon resonance features, confirming their nanoscale nature. Functional group analysis by FTIR indicated the role of phytochemical constituents in the reduction and stabilization of the bimetallic system. Elemental composition and morphological investigations using EDX and FESEM revealed that the synthesized Ag–Zn BMNPs possess predominantly spherical morphology and particle sizes ranging from 10 to 70 nm. The photocatalytic activity of the prepared nanoparticles was examined under natural sunlight irradiation for the degradation of methylene blue (MB), a representative organic dye contaminant. The influence of key operational parameters, including irradiation time, dye concentration, solution pH, and catalyst loading, was systematically assessed. Maximum degradation efficiency of 86.85% was achieved at neutral pH (7), with a catalyst dosage of 40 mg, an initial MB concentration of 5 ppm, and an exposure time of 180 min. The findings demonstrate that green-synthesized Ag–Zn bimetallic nanoparticles are promising photocatalysts for environmentally sustainable wastewater treatment applications.

1. Introduction

The discharge of dye-containing industrial effluents into water bodies poses a serious environmental concern due to their toxicity, persistence, and adverse effects on aquatic life. Methylene blue (MB), a widely used synthetic dye, is frequently detected in wastewater and requires effective removal strategies [1]. Photocatalytic degradation has emerged as a sustainable and efficient approach for dye remediation, particularly when driven by sunlight [2].

Nanostructured photocatalysts have gained considerable attention due to their large surface area and superior reactive properties; nevertheless, single-metal systems frequently exhibit poor light harvesting efficiency and fast recombination of photogenerated charge carriers [3]. To overcome these limitations, bimetallic nanoparticles have emerged as effective photocatalysts, benefiting from the cooperative effects between two different metals. Among them, Ag–Zn bimetallic nanoparticles are particularly attractive, as silver facilitates enhanced light absorption and electron mobility, whereas zinc promotes efficient charge separation, thereby improving overall photocatalytic activity [4].

Traditional fabrication routes for nanomaterials often rely on hazardous chemicals and require high energy input, raising environmental and safety concerns. In contrast, plant-mediated green synthesis offers a sustainable alternative [5] in which naturally occurring phytochemicals function as effective reducing and stabilizing agents. *Achyranthes aspera* (Apamarga), a widely distributed tropical medicinal weed known for its anti-inflammatory, antimicrobial, and diuretic properties [6], is rich in bioactive secondary metabolites that provide suitable functional groups for nanoparticle formation.

Journal of Chemical Health Risks
www.jchr.org
JCHR (2025) 15(5), 3495-3502 | ISSN:2251-6727

In the present investigation, a simple and eco-friendly approach is employed to synthesize Ag–Zn bimetallic nanoparticles using *Achyranthes aspera* leaf extract. The photocatalytic efficiency of the synthesized nanoparticles is examined under natural sunlight for the degradation of methylene blue, demonstrating their potential applicability in sustainable wastewater treatment processes.

This paper has mainly discussed the synthesis of Ag-Zn bimetallic nanoparticles from extracts of *Achyranthes aspera* leaves via the potent green reduction method. The synthesized nanoparticles were characterized and then applied for photocatalytic degradation of a commonly found organic dye, Methylene Blue (MB).

2. Materials and methods

2.1. Preparation of *Achyranthes aspera* leaf extract

The leaves were carefully detached from the stems and thoroughly cleaned by rinsing twice with running tap water to eliminate dust, debris, and surface contaminants, followed by two washes with double-distilled water. The cleaned leaves were shade-dried at room temperature for seven days. After drying, the leaves were finely chopped and ground into a uniform powder using a domestic blender. The resulting powder was stored in an airtight container and preserved at 4 °C in a refrigerator until further use. Leaf samples were collected during the morning hours on each day of analysis.

Fig 1: *Achyranthes aspera* plant

2.2 Synthesis of Ag-Zn bimetallic nanoparticles using leaf extract of *Achyranthes aspera*

An aqueous solution of $AgNO_3$ (10 mM) was prepared by dissolving 1.6987 g in 100 mL of distilled water, while $Zn(NO_3)_2{\cdot}6H_2O$ (10 mM) was separately prepared by dissolving 2.9079 g in 100 mL of distilled water. Eighty milliliters of filtered *Achyranthes aspera* leaf extract was first added to the silver nitrate solution, producing a pale yellow color. The zinc nitrate solution was then added dropwise under continuous stirring. The reaction mixture was stirred at 80 °C for 90 min and maintained at pH 8 using 0.1 N HCl or 0.1 N NH_4OH. A dark brown coloration confirmed the formation of Ag–Zn bimetallic nanoparticles. The nanoparticles were recovered by centrifugation at 5000 rpm for 50 min, washed thrice with deionized water, and dried at 70 °C for 3 h for further characterization.

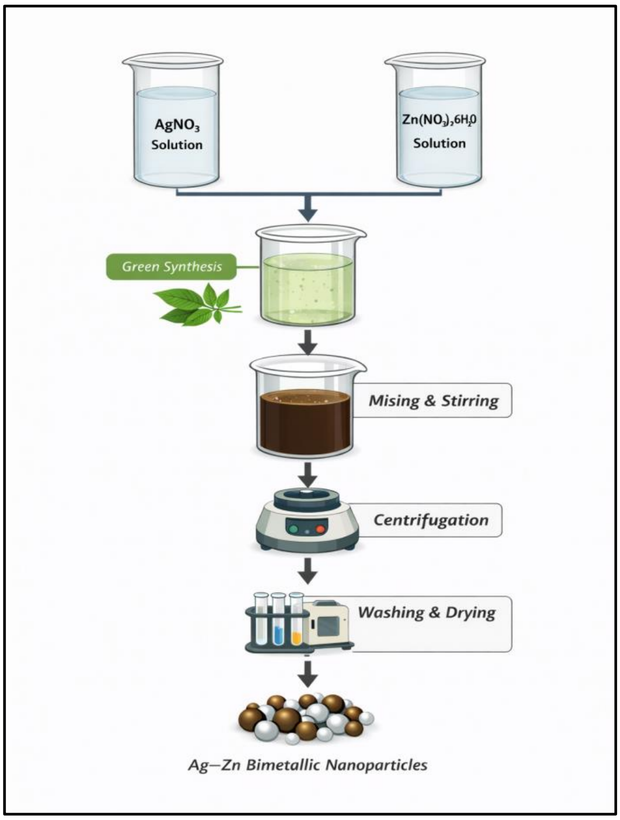

Fig 2: Schematic representation of the green synthesis of Ag–Zn BMNPs

2.3 Characterization

The development and characterization of Ag-Zn BMNPs were carried out using multiple analytical techniques: UV-Visible absorption spectroscopy (300–800 nm) with a UV2450 SHIMADZU double-beam spectrophotometer; FTIR analysis (4000–400 cm^{-1}) using a Bruker ALPHA II spectrometer; FESEM and EDX studies using a JSM-7100F (JEOL) instrument operated at 0.5–30 kV with magnifications from ×10 to ×1,000,000 and BET surface area analysis using a BELSORP MAX II instrument.

3. Results and Discussion

3.1. UV–Visible Spectral Analysis

Journal of Chemical Health Risks
www.jchr.org
JCHR (2025) 15(5), 3495-3502 | ISSN:2251-6727

The UV–Visible absorption spectrum of Ag–Zn BMNPs

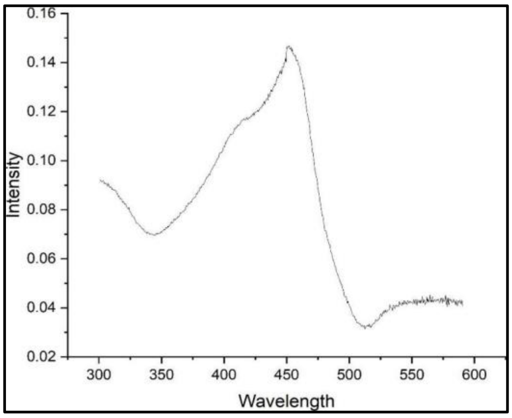

(Fig 3) exhibits a characteristic surface plasmon resonance (SPR) band at approximately 449 nm, confirming the nanoscale formation of the synthesized particles [7.

Fig 3: UV-Visible absorption spectrum of Ag-Zn BMNPs

3.2. FTIR spectroscopic analysis

FTIR analysis was employed to identify the functional groups associated with the biomolecules present in the *Achyranthes aspera* leaf extract. These biomolecules function as natural reducing and capping agents, facilitating the conversion of Ag^{+} and Zn^{2+} ions into their zero-valent forms (Ag^0 and Zn^0) and contributing to the stabilization of the synthesized Ag–Zn BMNPs. Prominent absorption bands were recorded and assigned by comparison with standard reference values to determine the functional groups present in both the plant extract and the green-synthesized Ag–Zn BMNPs. The FTIR spectrum of the Ag–Zn BMNPs prepared using *Achyranthes aspera* leaf extract is shown in Fig 4. and reveals the presence of phytochemical constituents such as terpenes, flavonoids, polyphenols, glycosides, carbohydrates, tannins, amides, amines, and sterols on the surface of the nanoparticles.

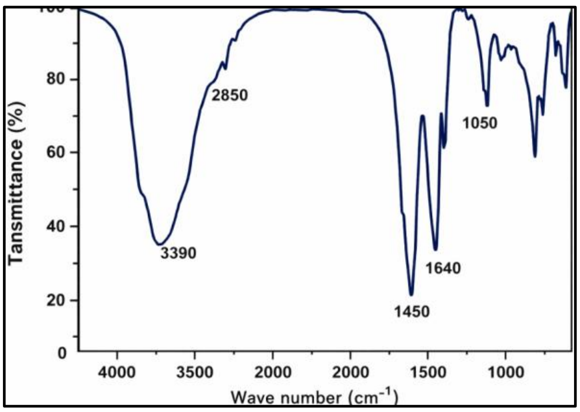

Fig 4: FTIR spectrum of Ag-Zn BMNPs

The N-H stretching vibrations of amines and O-H stretching vibrations of hydroxyl groups of alcohols and phenols are shown by prominent broad peak location at 3390 cm^{-1}, in the FTIR spectrum of Ag-Zn BMNPs. The C=O stretching of the amide group results in a strong peak at 1640 cm^{-1}. C-H stretching is observed at 2850 cm^{-1} and C-O stretching in is seen by the sharp peak at 1050 cm^{-1} and the peak at 1450 cm^{-1} is due to C-H bending vibrations [8].

Because the phytomolecules in the leaf extract act as bio reducing agents, capping and stabilizing agents for the produced nanoparticles, FTIR analysis clearly confirms that all of the previously mentioned absorption peaks of the leaf extract are barely shifted in the FTIR spectrum of Ag-Zn BMNPs. Biodegradable, well- Capping distributed, bio-soluble, biocompatible, and non-toxic capping agents are ideal. agents improve the biological characteristics of nanoparticles. The presence of these IR peaks in Ag-Zn BMNPs demonstrated that plant secondary metabolites such as carbohydrates, glycosides, Saponin, phytosterols, phenols, tannins, flavonoids, proteins, amino acids, terpenoids, carboxylic acids, amides, carbonyl compounds, and alkyl were present on the nanoparticles surface.

3.3. Field Emission Scanning Electron Micrographs (FESEM) and EDX analysis

Energy-dispersive X-ray (EDX) analysis was employed to determine the elemental constituents of the BMNPs synthesized using *Achyranthes aspera* leaf extract. The EDX spectrum and corresponding elemental composition are presented in Fig 5 and Table 1, respectively. The results confirm the presence of silver and zinc, verifying the successful formation of Ag–Zn bimetallic nanoparticles. The EDX data also provide quantitative information on the relative amounts of these elements in the BMNPs. A noticeable oxygen signal suggests that a portion of the nanoparticles may exist as Ag–Zn oxides, which can be attributed to the open reaction conditions during synthesis. FESEM micrographs of the Ag–Zn BMNPs at various magnifications are shown in Fig 6, revealing particle sizes in the range of 83-105 nm. The formation of relatively small nanoparticles highlights the effective reducing capability of the *Achyranthes aspera* leaf extract in the green synthesis of bimetallic nanoparticles.

Table 1: Quantitative results of Ag-Zn BMNPs

Journal of Chemical Health Risks
www.jchr.org
JCHR (2025) 15(5), 3495-3502 | ISSN:2251-6727

Element	Weight %	Atomic %
Zn	33.93	49.80
Ag	56.23	40.10
O	10.84	10.10
Totals	100.0	100.0

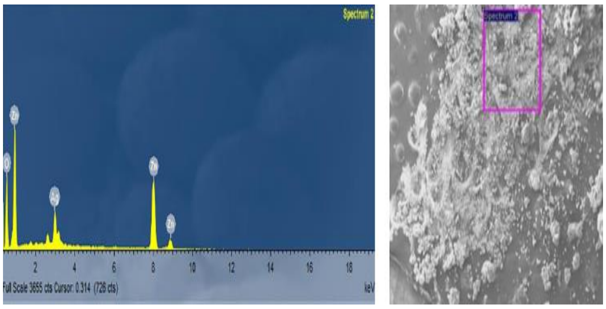

Fig 5: EDX analysis of Ag-Zn BMNPs

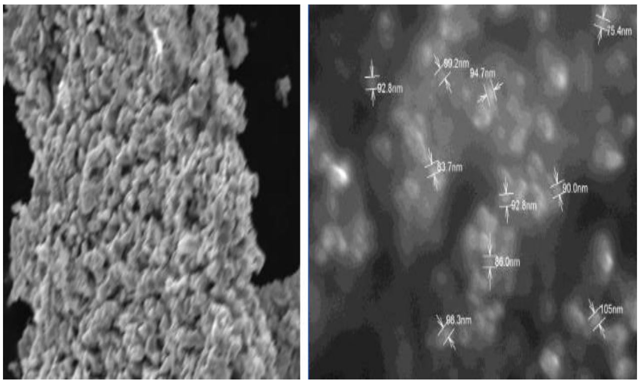

Fig 6: FESEM images of Ag-Zn BMNPs

3.4. BET analysis

The adsorption–desorption isotherm obtained from the graph corresponds to a Type II isotherm. The relatively flat region observed in the central portion of the curve indicates the development of a monolayer on the adsorbent surface. According to the BET theory, a Type II isotherm is observed when the constant *c* is greater than unity. At very low relative pressures, nitrogen molecules initially occupy the micropores. The point of inflection, known as the knee region, signifies the onset of monolayer coverage, followed by multilayer adsorption as the pressure increases [9]. At higher relative pressures, capillary condensation becomes prominent. Thus, adsorption proceeds through successive multilayer formation and capillary condensation, which is characteristic of a Type II isotherm. The specific surface area of the synthesized bimetallic nanoparticles was calculated to be 8.289 × 10^{18} m^2/g, indicating a high surface area. Consequently, these BMNPs are well suited for catalytic applications due to the availability of abundant active surface sites.

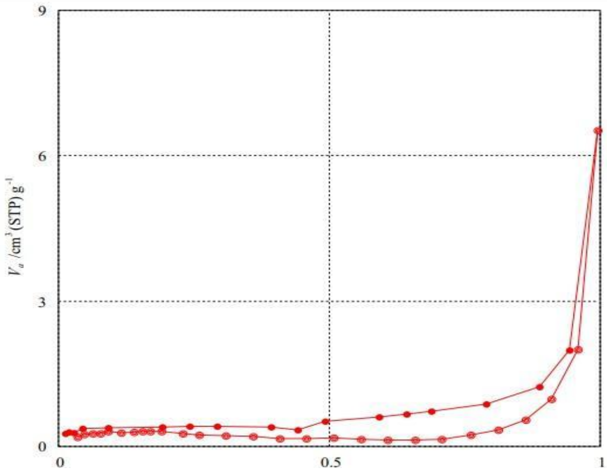

Fig 7: Adsorption/Desorption isotherm of Ag-Zn Bimetallic nanoparticles

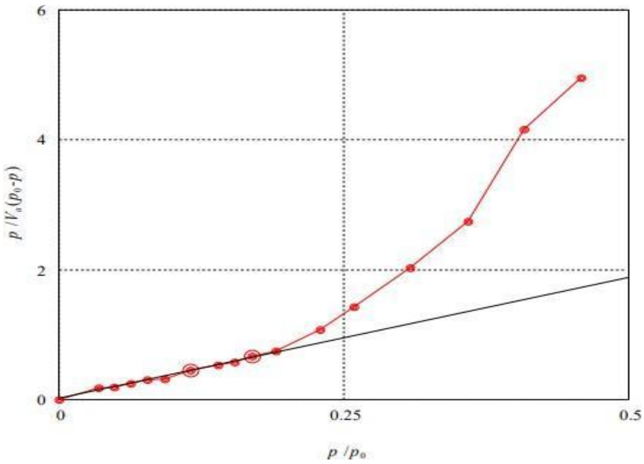

Fig 8: BET isotherm of Ag-Zn Bimetallic nanoparticles

3.5. Photocatalytic degradation of methylene blue

A concentrated methylene blue stock solution (50 ppm) was initially prepared and subsequently diluted to obtain working solutions with concentrations ranging from 5 to 35 ppm. For each experiment, measured amounts of Ag–Zn bimetallic nanoparticles (10–70 mg) were dispersed in 100 mL of the dye solution. The pH of the reaction mixtures was adjusted within the range of 4–11 using 0.1 N hydrochloric acid or 0.1 N sodium hydroxide solutions. Prior to irradiation, the suspensions were magnetically stirred in the dark for 20 min to achieve adsorption–

Journal of Chemical Health Risks
www.jchr.org
JCHR (2025) 15(5), 3495-3502 | ISSN:2251-6727

desorption equilibrium between the dye molecules and the photocatalyst surface.

Photocatalytic degradation studies were conducted under natural sunlight between 10:00 a.m. and 1:00 p.m., with ambient temperatures varying from 34 to 39 °C. At regular intervals of 30 min, aliquots were collected and centrifuged to remove the photocatalyst. The resulting clear supernatant was analyzed using a UV–Visible spectrophotometer. Absorbance measurements were recorded while systematically varying parameters such as irradiation time, pH, initial dye concentration, and catalyst dosage. Methylene blue showed a characteristic absorption maximum at 668 nm, and the degradation efficiency was evaluated by calculating the percentage of photodegradation using the appropriate relation [10].

$$\% \text{ degradation} = (A_0 - A_t)/A_0 \times 100$$

Where A0 is the initial absorbance of the MB solution at zero minutes and At is the absorbance of the degraded solution after time t minutes.

The UV-visible spectrophotometer was used to investigate the photocatalytic activity of Ag-Zn BMNPs in the methylene blue visible region of the light source. The absorption spectrum of a 10-ppm methylene blue solution showed maximum absorption peak at 668 nm, and this maximum absorption peak was used to monitor the photodegradation reaction of MB dye for the rest of the research.

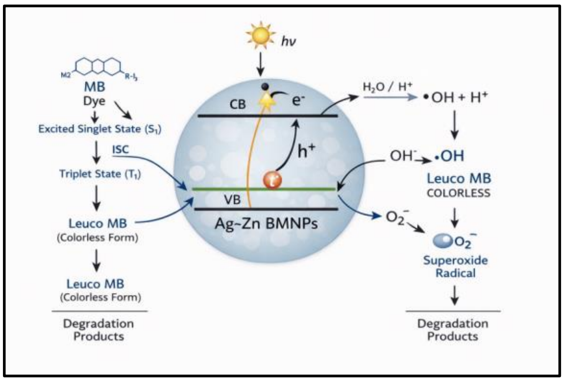

Fig 9: Photocatalytic degradation mechanism of MB dye

MB dye enters its first excited singlet state by absorbing sufficient wavelength photons. It then enters the triplet state after experiencing intersystem crossing (ISC). Ag-Zn BMNPs absorb the radiation in the meantime in order to stimulate their electron from the valence band to the conduction band [11]. To create, the hole takes an electron from H2O, H^+ ion, and the OH radicals are formed. The ·OH radical oxidizes the MB dye to its leuco form degrading it into a colorless product. An O2 molecule will tap the electron, resulting in the formation of a superoxide anion radical ($.O^{2-}$). The methylene blue dye is converted to its leuco form by the generated anion radical, which then degrades to produce products.

3.5.1. The impact of interaction time

The photocatalytic efficiency of Ag–Zn bimetallic nanoparticles toward the degradation of methylene blue dye was evaluated under natural sunlight using batch experimental conditions. An increase in photocatalytic performance was anticipated with prolonged contact between the dye molecules and the catalyst. To examine the influence of irradiation time, experiments were conducted using 100 mL of a 10 ppm methylene blue solution with a catalyst dosage of 10 mg of Ag–Zn BMNPs at neutral pH (pH 7). The corresponding results are illustrated in Fig 11.

During the initial phase of the reaction, up to 120 minutes, a sharp increase in the percentage of dye degradation was observed. Beyond this duration, although the degradation continued to increase, the rate became comparatively slower, resulting in a less pronounced slope while still maintaining substantial degradation efficiency.

These observations indicate that the photocatalytic degradation of methylene blue proceeds rapidly within the first 120 minutes, after which the reaction rate decreases but remains effective up to 180 minutes. The accelerated degradation at earlier stages can be attributed to the abundance of available active sites on the BMNPs surface, which promotes strong adsorption of dye molecules. After prolonged exposure, equilibrium between occupied and unoccupied adsorption sites is gradually achieved [12], leading to a reduced yet sustained rate of photocatalytic degradation.

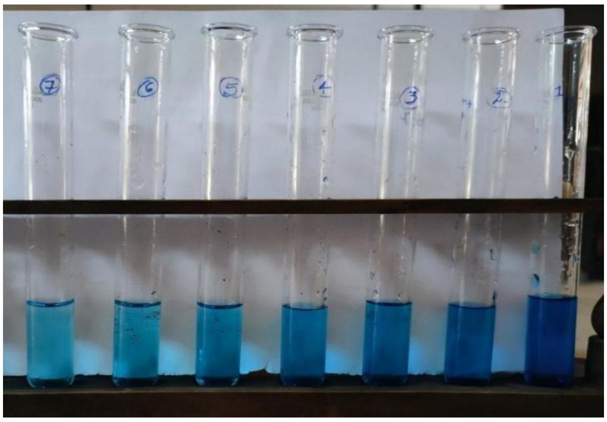

(1) 0 mins (2) 30 mins (3) 60 mins
(4) 90 mins (5) 120 mins (6) 150
mins (7) 180 mins

Fig 10: MB dye on photodegradation at different time intervals

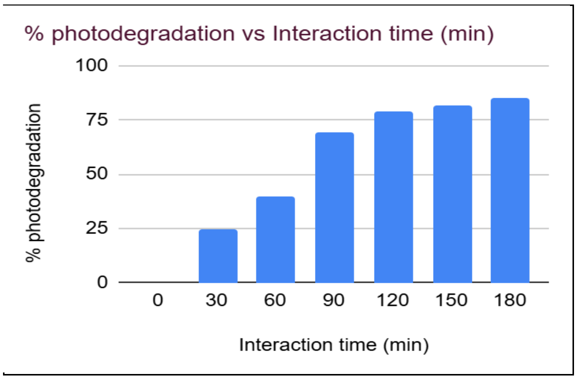

Fig 11: Effect of interaction time on photodegradation

3.5.2. Effect of initial concentration of MB dye solution

The initial concentration of methylene blue is an important factor influencing the photocatalytic degradation rate. To evaluate this effect, the amount of Ag–Zn BMNPs used as the photocatalyst was fixed at 10 mg, the solution pH was maintained at 7, and the irradiation period was set to 180 minutes. Photodegradation experiments were carried out using methylene blue solutions of varying initial concentrations, namely 5, 10, 15, 20, 25, 30, and 35 ppm. The variation in degradation efficiency with respect to dye concentration is illustrated in Fig 12. The results indicate that maximum photodegradation efficiency was achieved at the lowest dye concentration (5 ppm), while a progressive decline in degradation efficiency was observed as the initial concentration increased.

This reduction in photocatalytic performance at higher dye concentrations can be attributed to the shielding effect of excess dye molecules, which limits the penetration of incident light [13] to the surface of the Ag–Zn BMNPs. Consequently, reduced photon availability at the catalyst surface leads to a decrease in the percentage of photodegradation.

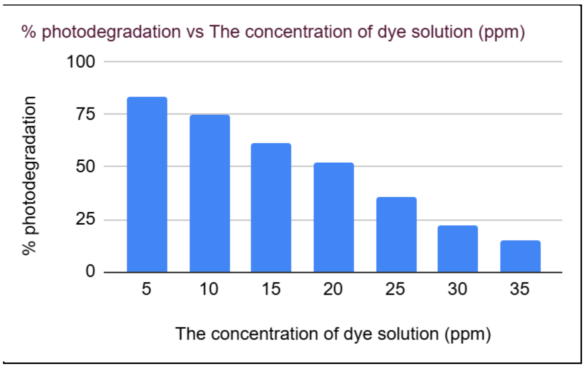

Fig 12: Effect of concentration of MB dye solution on photodegradation

3.5.3. Effect of pH

The pH of the dye solution plays a crucial role in controlling the adsorption behavior of methylene blue on the photocatalyst surface. To investigate this effect, the initial concentration of methylene blue was fixed at 10 ppm, and the catalyst dosage was maintained at 10 mg during irradiation. Reaction mixtures with pH values ranging from 4 to 11 were prepared for the study. The corresponding degradation efficiencies are summarized in Fig 13.

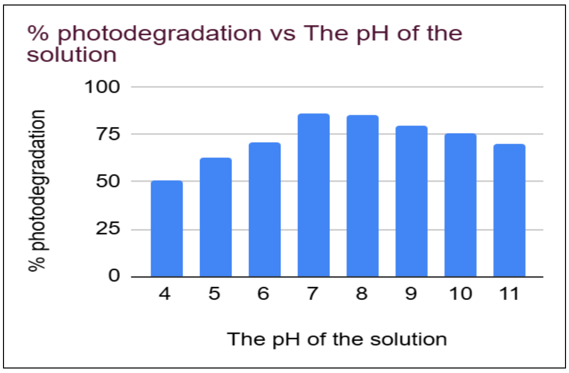

Fig 13: Effect of pH on photodegradation

The results indicate that photocatalytic degradation was minimal under acidic conditions. In such environments, the presence of excess hydrogen ions competes with the cationic methylene blue molecules for active adsorption sites on the catalyst surface, leading to reduced dye uptake and lower degradation efficiency [14]. In contrast, at pH values above 7, enhanced degradation was observed in alkaline media. This improvement can be attributed to the increased concentration of hydroxyl ions, which impart a negative charge to the catalyst surface and thereby promote stronger electrostatic attraction between the photocatalyst and the positively charged methylene blue molecules, resulting in significantly higher removal efficiency.

3.5.4. Effect of dosage of photocatalyst

In photocatalytic dye degradation, the amount of catalyst employed is a critical factor influencing decolorization efficiency. To avoid unnecessary consumption of costly catalyst materials while ensuring effective photon absorption, optimization of the photocatalyst dosage is required. Accordingly, the catalyst loading was systematically varied from 10 mg to 70 mg in 100 mL of a 10 ppm methylene blue solution maintained at pH 8 under irradiation conditions.The corresponding percentage degradation of methylene blue for different catalyst dosages is presented is illustrated in Fig 14.

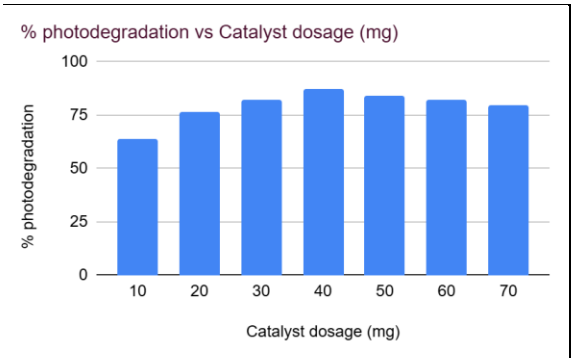

Fig 14: Effect of dosage of catalyst on photodegradation

The results indicate that increasing the photocatalyst dosage from 10 mg to 40 mg in 100 mL of solution led to a noticeable enhancement in the degradation of methylene blue. This improvement can be attributed to the higher availability of active surface sites, which promotes the generation of reactive species responsible for dye breakdown. However, further increases in catalyst loading beyond this optimum level resulted in a decline in degradation efficiency.

The reduction in performance at higher catalyst dosages can be explained by the formation of increasingly turbid suspensions, which hinder effective light penetration into the reaction medium [15]. In addition, excessive catalyst loading promotes particle agglomeration and sedimentation, thereby reducing the effective active surface area accessible for photocatalytic reactions and ultimately lowering the degradation efficiency.

Conclusions

An environmentally benign approach was employed for the synthesis of silver–zinc bimetallic nanoparticles using *Achyranthes aspera* leaf extract. UV–Visible spectroscopic analysis confirmed the formation of nanoparticles through the appearance of characteristic surface plasmon resonance bands, indicating their nanoscale dimensions. FTIR spectroscopy revealed the involvement of phytochemical constituents acting as both reducing and stabilizing agents during nanoparticle formation. Morphological and elemental analyses using FESEM and EDX demonstrated that the synthesized Ag–Zn BMNPs possess predominantly spherical shapes with particle sizes ranging from 10 to 70 nm.

The photocatalytic performance of the synthesized nanoparticles was evaluated under natural sunlight for the degradation of methylene blue, a commonly encountered environmental contaminant. The degradation efficiency was found to be strongly influenced by operational parameters such as irradiation time, initial dye concentration, solution pH, and photocatalyst dosage. Based on systematic optimization studies, the most favorable conditions for methylene blue degradation were identified as pH 7, a catalyst loading of 40 mg, a dye concentration of 5 ppm, and a contact time of 180 minutes. Under these optimized conditions, a maximum photodegradation efficiency of 86.85% was achieved.

References

1. Setien, E., Monti, G. A., Moyano, F., & Acevedo, D. (2025). Green Nanotechnology for Water Remediation: Eco-Friendly Synthesis of Zinc Oxide Nanoparticles and Methylene Blue Degradation Kinetics. *Langmuir*.
2. Alzahrani, E. A., Nabi, A., Kamli, M. R., Albukhari, S. M., Althabaiti, S. A., Al- Harbi, S. A., ... & Malik, M. A. (2023). Facile green synthesis of ZnO NPs and plasmonic Ag-supported ZnO nanocomposite for photocatalytic degradation of methylene blue. *Water*, *15*(3), 384.
3. Dutta, K. (2021). Metal oxides as decontaminants of water and wastewater. In *Metal, Metal-Oxides and Metal-Organic Frameworks for Environmental Remediation* (pp. 1-28). Cham:

Springer International Publishing.

4. Liu, Y., Zhang, Q., Xu, M., Yuan, H., Chen, Y., Zhang, J., ... & You, B. (2019). Novel and efficient synthesis of Ag-ZnO nanoparticles for the sunlight-induced photocatalytic degradation. *Applied surface science*, *476*, 632-640.

5. El Shafey, A. M. (2020). Green synthesis of metal and metal oxide nanoparticles from plant leaf extracts and their applications: A review. *Green Processing and Synthesis*, *9*(1), 304-339.

6. Talreja, S., & Tiwari, S. (2023). A comprehensive review of Achyranthes aspera: Ethnopharmacology, phytochemistry, and therapeutic potential. *An Int. J. Research in AYUSH and Allied Systems*, *10*(5), 270-278.

7. Anjum, S., Khan, A. K., Qamar, A., Fatima, N., Drouet, S., Renouard, S., ... & Hano, C. (2021). Light tailoring: Impact of UV-C irradiation on biosynthesis, physiognomies, and clinical activities of Morus macroura-mediated monometallic (Ag and ZnO) and bimetallic (Ag–ZnO) nanoparticles. *International journal of molecular sciences*, *22*(20), 11294.

8. Mazhar, T. (2022). Bio-assisted synthesis of bi-metallic (Ag-Zn) nanoparticles by leaf extract of Azadirachta indica and its antimicrobial properties. *International Journal of Nano Dimension*, *13*(2).

9. Pham, T. A. T., Tran, V. A., Le, V. D., Nguyen, M. V., Truong, D. D., Do, X. T., & Vu, A. T. (2020). Facile preparation of ZnO nanoparticles and Ag/ZnO nanocomposite and their photocatalytic activities under visible light. *International Journal of Photoenergy*, *2020*(1), 8897667.

10. Alharthi, F. A., Alanazi, H. S., Alotaibi, K. M., & Ahmad, N. (2022). Photodegradation of methylene blue and Rose Bengal employing g-C3N4/ZnWO4 nanocatalysts under ultraviolet light irradiation. *Journal of Nanoparticle Research*, *24*(6), 125.

11. Tahir, M. B., Iqbal, T., Rafique, M., Rafique, M. S., Nawaz, T., & Sagir, M. (2020). Nanomaterials for photocatalysis. In *Nanotechnology and photocatalysis for environmental applications* (pp. 65-76). Elsevier.

12. Al-Mamun, M. R., Islam, M. S., Hossain, M. R., Kader, S., Islam, M. S., & Khan, M. Z. H. (2021). A novel and highly efficient Ag and GO co-synthesized ZnO nano photocatalyst for methylene blue dye degradation under UV irradiation. *Environmental Nanotechnology, Monitoring & Management*, *16*, 100495.

13. Rafaie, H. A., Nor, R. M., Azmina, M. S., Ramli, N. I. T., & Mohamed, R. (2017). Decoration of ZnO microstructures with Ag nanoparticles enhanced the catalytic photodegradation of methylene blue dye. *Journal of environmental chemical engineering*, *5*(4), 3963-3972.

14. Trieu, Q. A., Le, C. T. B., Pham, C. M., & Bui, T. H. (2023). Photocatalytic degradation of methylene blue and antibacterial activity of silver nanoparticles synthesized from Camellia sinensis leaf extract. *Journal of Experimental Nanoscience*, *18*(1), 2225759.

15. Guo, Y., Fu, X., Liu, R., Chu, M., & Tian, W. (2022). Efficient green photocatalyst of Ag/ZnO nanoparticles for methylene blue photodegradation. *Journal of Materials Science: Materials in Electronics*, *33*(5), 2716-2728.